

# Hypoxia-induced cell death in human malignant glioma cells: energy deprivation promotes decoupling of mitochondrial cytochrome *c* release from caspase processing and necrotic cell death

JP Steinbach<sup>\*1</sup>, H Wolburg<sup>2</sup>, A Klumpp<sup>1</sup>, H Probst<sup>3</sup> and M Weller<sup>1</sup>

<sup>1</sup> Laboratory of Molecular Neuro-Oncology, Department of Neurology, University of Tübingen, School of Medicine, Tübingen, Germany

<sup>2</sup> Institute of Pathology, Division of Molecular Pathology, University of Tübingen, School of Medicine, Tübingen, Germany

<sup>3</sup> Institute of Physiological Chemistry, University of Tübingen, Germany

\* Corresponding author: JP Steinbach, Laboratory of Molecular Neuro-Oncology, Department of Neurology, University of Tübingen, Medical School, Hoppe-Seyler-Strasse 3, 72076 Tübingen, Germany. Tel: +49-7071-2982141; Fax: +49-7071-295260; E-mail: joachim.steinbach@uni-tuebingen.de

Received 26.6.02; revised 9.1.03; accepted 10.3.03

Edited by JA Cidlowski

## Abstract

Hypoxia induces apoptosis in primary and transformed cells and in various tumor cell lines *in vitro*. In contrast, there is little apoptosis and predominant necrosis despite extensive hypoxia in human glioblastomas *in vivo*. We here characterize ultrastructural and biochemical features of cell death in LN-229, LN-18 and U87MG malignant glioma cells in a paradigm of hypoxia with partial glucose deprivation *in vitro*. Electron microscopic analysis of hypoxia-challenged glioma cells demonstrated early stages of apoptosis but predominant necrosis. ATP levels declined during hypoxia, but recovered with re-exposure to normoxic conditions unless hypoxia exceeded 8 h. Longer hypoxic exposure resulted in irreversible ATP depletion and delayed cell death. Hypoxia induced mitochondrial release of cytochrome *c*, but there was no cleavage of caspases 3, 7, 8 or 9, and no DNA fragmentation. Ectopic expression of BCL-X<sub>L</sub> conferred protection from hypoxia-induced cell death, whereas the overexpression of the antiapoptotic proteins X-linked-inhibitor-of-apoptosis-protein and cytokine response modifier-A had no effect. These findings suggest that glioma cells resist adverse effects of hypoxia until energy stores are depleted and then undergo necrosis rather than apoptosis because of energy deprivation.

*Cell Death and Differentiation* (2003) 10, 823–832. doi:10.1038/sj.cdd.4401252

**Keywords:** glioma; hypoxia; apoptosis; necrosis; cytochrome *c*; caspase; BCL-X<sub>L</sub>; ATP

**Abbreviations:** APAF 1, apoptotic protease activating factor 1; CD95L, CD95 ligand; Crm-A, cytokine response modifier-A; ECL, enhanced chemiluminescence; GFP, green fluorescent protein; TUNEL, terminal dUTP *in situ* nick end-labeling; VEGF, vascular endothelial growth factor; XIAP, X-linked-inhibitor-of-apoptosis-protein.

## Introduction

Extensive hypoxia is a hallmark of glioblastoma and other solid tumors.<sup>1–3</sup> Already at early stages of tumorigenesis, tumor hypoxia may be precipitated by regression of co-opted host vasculature, resulting in hypoxic tumor cell death and thus selective pressure for hypoxia-resistant clones.<sup>4,5</sup> Ultimately, however, the remaining tumor is rescued by robust angiogenesis at the tumor margin. In established tumors, chronic hypoxia is caused by increased metabolic activity and rapid tumor cell growth outscaling tumor neoangiogenesis and compromising the vascular supply of oxygen and nutrients. In addition, acute tumor hypoxia can be brought about by tumor vessel occlusion via thrombosis<sup>6,7</sup> or by fluctuations in the oxygenation of disordered tumor vasculature.<sup>8,9</sup> Further, antiangiogenic therapeutic strategies can result in hypoxia and tumor cell death.<sup>10,11</sup>

Tumor hypoxia is relevant for (i) the selection of clones resistant to hypoxia-induced cell death and (ii) the biological behavior and response to therapy of the hypoxic tumor cell fraction. Hypoxia-induced cell death in E1A and Ha-*ras*-transformed cell lines,<sup>12</sup> several nonglioma tumor cell lines<sup>13,14</sup> and nontransformed cells<sup>15</sup> may take place predominantly by apoptosis *in vitro*. In contrast, glioblastoma cell death *in vivo* is predominantly necrotic,<sup>7,16</sup> while the amount of apoptosis is generally low.<sup>17</sup> Apoptotic changes defined by DNA strand breaks detected by terminal dUTP *in situ* nick end-labeling (TUNEL) are predominantly located among pseudopalisading perinecrotic cells<sup>18,19</sup> which express vascular endothelial growth factor (VEGF),<sup>20</sup> suggesting focal areas of hypoxia and a graded response of glioma cells to hypoxia. The small amount of apoptosis despite extensive tumor hypoxia suggests the development of resistance to hypoxia-induced apoptosis in glioblastomas by alterations in the cell death pathway including both short-term effects such as upregulation of antiapoptotic proteins<sup>21</sup> and genetic selection for cells with defects in the apoptotic pathway.<sup>12,22,23</sup> The apparent resistance to hypoxia-induced cell death translates also into clinical relevant adverse outcomes, since there is a worse prognosis for patients with extensively hypoxic solid tumors,<sup>6,24</sup> while both a higher amount of apoptosis and a low ratio of proliferation to apoptosis in glioblastomas may indicate a better prognosis.<sup>25,26</sup>

We here characterized the mode and biochemical features of hypoxia-induced cell death in malignant glioma cell lines *in vitro*. To model realistic conditions of the tumor microenvironment, we restricted glucose concentration in the medium to 2 mM for the hypoxic incubations, since many experimental studies have shown similar decreases in glucose concentration in the center of solid tumors in parallel to increasing hypoxia.<sup>27–29</sup> In particular, we studied ATP levels during hypoxia, since the mode of cell death can be ATP-dependent, with ATP acting as a molecular switch between apoptosis and necrosis in some paradigms.<sup>30,31</sup>

## Results

### Predominant necrosis and abortive apoptotic changes in hypoxia-induced cell death

The morphological features of hypoxia-induced glioma cell death were characterized by electron microscopy (EM). Primarily, cell death after hypoxia followed by normoxic recovery for 24 h with replenishment of glucose was studied. In the LN-229 cell line, there were only few cells which displayed apoptotic features at early time points, including cytoplasmic blebbing, nuclear chromatin condensation and margination with rare formation of apoptotic bodies. Necrotic changes, including mitochondrial swelling and organelle disruption, cytoplasmic vesiculation, vacuolization and rupture of the cell membrane at later time points were predominant (Figure 1a–d). In U87MG cells, early apoptotic changes were more pronounced, and cytoplasmic integrity was better preserved in the initial stages. However, at later time points, there was necrosis similar to LN-229 cells (Figure 1e–h). LN-229 cells were prepared for EM also directly following hypoxia of 8, 12 and 16 h to analyze early morphological changes. There were necrotic changes similar to those described above, but nuclear chromatin condensation and margination were less pronounced (cells exposed to hypoxia for 16 h are shown in Figure 1i). For comparison of typical apoptotic changes, LN-229 cells were exposed to (CD95 ligand) CD95L in a parallel experiment (Figure 1j).

In LN-18 cells, the morphological consequences of hypoxia occurred earlier than in LN-229 and U87MG cells. To investigate the time course of cell death induction, LN-18 cells were fixed for electron microscopy directly after hypoxia (Figure 2a–d) or after a 24 h period of normoxic recovery (Figure 2e–h). Compared with the morphology seen immediately after hypoxia, more prominent early apoptotic features developed in a delayed fashion after 8 and 12 h of hypoxia and subsequent further culturing at normoxia, with nuclear chromatin condensation and formation of apoptotic bodies in some cells. As in the LN-229 and U87MG cell lines, necrotic changes prevailed at later time points, ultimately leading to cell membrane disruption. The classical ultrastructural end stages of apoptosis (pyknotic cells with fragmented nuclei and apoptotic bodies, preserved cell membrane) which occur in these cells after treatment with death ligands, Teniposide (VM26), or other stimuli as described in previous studies<sup>32–34</sup> did not develop in either cell line during hypoxia-induced cell death.

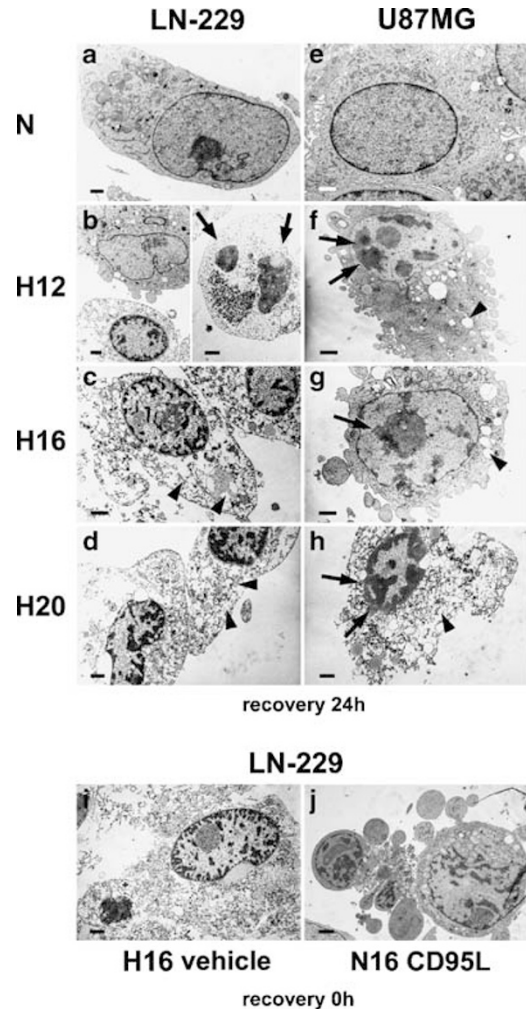


**Figure 1** Ultrastructural features of hypoxia-induced cell death in LN-229 and U87MG malignant glioma cells. (a–h) The cells were exposed to normoxia or hypoxia and 24 h normoxic recovery and prepared for electron microscopy. (a,e) Normoxic LN-229 and U87MG cells (N). (b–d) LN-229 cells exposed to hypoxia for 12–20 h. Note the features of early apoptotic death with cytoplasmic blebbing (upper cell in b), nuclear chromatin condensation (b–d) and margination (b, left panel, lower cell) and occasional formation of apoptotic bodies (B, right panel, arrows) as well as early and prominent necrotic changes with disruption of organelle integrity and cytoplasmic vesiculation and vacuolization (arrowheads in c,d). (f,g,h) U87MG cells exposed to hypoxia for 12–20 h. Cytoplasmic blebbing (f,g), nuclear chromatin condensation (arrows in f–h) and margination (h) are present in some cells, as well as disruption of organelle integrity, cytoplasmic vesiculation and vacuolization (arrowheads in F,G,H) at later stages. (i, k) LN-229 cells were exposed to hypoxia for 16 h (i) or to 100 U/ml CD95L for 16 h under normoxia (f) and were prepared for electron microscopy immediately thereafter (scale bar=1 μM)

### No specific Annexin V binding occurs during hypoxic cell death

To further characterize the mode of hypoxic cell death in this paradigm, Annexin V binding assays were performed in LN-18 and LN-229 cells. No specific apoptotic changes (i.e. Annexin V binding in cells not taking up propidium iodide, lower right quadrant) were detected. Some propidium iodide positive cells also stained positive for Annexin V, a finding consistent

with necrosis (upper right quadrant). Results in LN-18 cells stained immediately after hypoxia are shown in Figure 3. Similar results were obtained with LN-229 cells and after additional normoxic recovery (not shown).

### Progressive ATP depletion during hypoxia determines hypoxic cell death

To analyze cellular energy homeostasis during hypoxia and subsequent normoxic recovery of glioma cells, ATP levels

were monitored in LN-229 cells and correlated with cell death as assessed by LDH release. At 4 and 8 h of hypoxia, cellular ATP levels were reduced, but recovered during additional normoxic incubation with glucose supplementation (Figure 4a). While cell death took place during hypoxia (white bars in Figure 4b), there was no further delayed cell death during the recovery period following 4 and 8 h of hypoxia (black bars in Figure 4b). In contrast, ATP stores were irreversibly depleted at 12 h of hypoxia and at later time points, and delayed cell death occurred.

### Hypoxic cell death is dependent on glucose concentration

To define the threshold for glucose concentrations in the medium necessary for survival under hypoxic conditions, LN-229 cells were incubated under hypoxia with glucose concentrations of 2 mM, 5 mM and full serum-free medium (25 mM glucose). At a starting concentration of 2 mM, glucose was less than 1 mM at H8, where significant cell death emerged (Figure 5a). 25 mM and 5 mM glucose in the media protected the cells from hypoxia-induced cell death (Figure 5b,c). In addition, glucose concentrations above 2 mM protected against hypoxia-induced ATP depletion as described previously<sup>35</sup> and cytochrome *c* release (data not shown).

### Mitochondrial cytochrome *c* release fails to promote caspase processing during hypoxia-induced cell death

To characterize the hypoxia-induced cell death pathway at a biochemical level, mitochondrial cytochrome *c* release, caspase processing and DNA fragmentation were examined as three salient features typically accompanying apoptosis. There was pronounced cytochrome *c* release from mitochondria into the cytosol from H8 on in LN-229 cells (Figure 6a). Similar results were obtained in LN-18 and U87MG cells (not shown). Swelling of mitochondria with distortion of the cristae was observed in LN-229 cells exposed to hypoxia for 8 h and immediately thereafter prepared for electron microscopy as a possible morphological correlate of mitochondrial injury (Figure 6b). In contrast to other models of cell death, the observed release of cytochrome *c* failed to promote the processing of caspases 3, 7, 8 and 9 during hypoxia-induced cell death in LN-18 cells. In contrast, caspase cleavage was

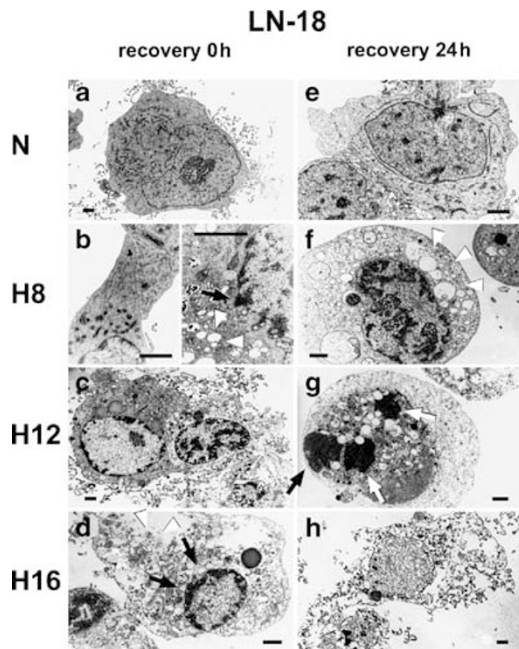


**Figure 2** Ultrastructural features of hypoxia-induced cell death in LN-18 malignant glioma cells. The cells were incubated under normoxia or hypoxia for 8, 12 or 16 h and prepared either immediately for electron microscopy to detect early morphological changes (a-d), or after 24 h of normoxic recovery (e-h). (a,d) Normoxic cells (N). (b-d) LN-18 cells fixed directly after hypoxia. Note the primary cytoplasmic damage with vesiculation and vacuolization (arrowheads in b and d) and a lesser degree of nuclear changes with nuclear indentations (arrows in b) and some chromatin condensation (arrows in d). (f-h) LN-18 cells fixed 24 h after recovery from hypoxia. Early apoptotic changes are emerging only in some cells, with nuclear chromatin condensation (shown in f) in parallel with cytoplasmic vesiculation and vacuolization (arrowheads in f) and rare formation of apoptotic bodies (arrows in g). Necrosis (arrows in g). Necrosis (arrows in g). Necrosis as described above is prominent at later time points (H). (scale bar=1  $\mu$ M)

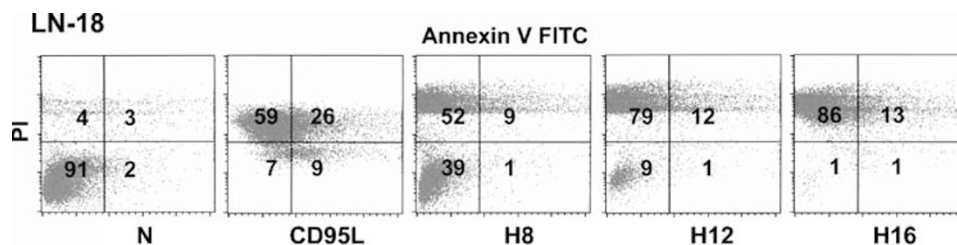


**Figure 3** Annexin V binding in hypoxia-induced cell death. LN-18 cells were exposed to normoxia or hypoxia and analyzed immediately thereafter for Annexin V binding and propidium iodide uptake (PI). LN-18 cells exposed to CD95L in the presence of cycloheximide were employed as positive controls. No Annexin V binding in viable cells not taking up PI was observed in hypoxia-induced cell death, indicating the absence of apoptosis

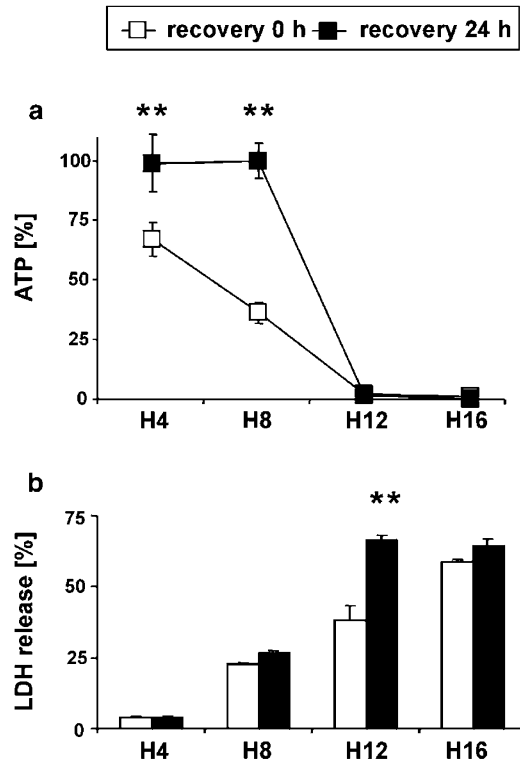


**Figure 4** Irreversible ATP depletion precedes delayed hypoxia-induced cell death. LN-229 cells were exposed to normoxia or hypoxia and either analyzed immediately or after 24 h of normoxic recovery. (a) Cellular ATP content was determined by luciferase assay. (b) In a parallel assay, cell death was assessed by LDH release (\*\* $P < 0.01$  for the comparison of recovery 0 h versus recovery 24 h after hypoxia, Student's *t*-test)

readily induced by CD95L (Figure 6c). Similar results were obtained in LN-229 and U87MG cells (data not shown). Further, hypoxia did not generate DEVD-amc-cleaving caspase activity corresponding to the processing of caspases 3 or 7 (Figure 6d). DNA fragmentation, a downstream consequence of caspase activity mediated by DNA fragmentation factor (DFF) 45, was not detectable in LN-229 cells after hypoxia. In contrast, basal DNA fragmentation under normoxic conditions decreased following 12 and 16 h of hypoxia (Figure 6e). The absence of caspase cleavage, DNA fragmentation and late-stage apoptotic morphology suggested that the apoptotic cascade was largely disabled at the step of cytochrome *c*-dependent caspase processing.

### Ectopic expression of BCL-X<sub>L</sub> protects glioma cells from hypoxia-induced cell death

Although mitochondrial damage and the release of cytochrome *c* are commonly modulated by BCL-2 family proteins, the protein levels of BCL-2, BCL-X<sub>L</sub> and BAX remained unchanged during hypoxia (data not shown). BCL-X<sub>L</sub> has been shown to protect from hypoxic cell death, and previous work from our laboratory has shown that ectopic expression of BCL-X<sub>L</sub> in LN-18 and LN-229 cells also inhibits death receptor-mediated apoptosis presumably by preventing mitochondrial cytochrome *c* release.<sup>36</sup> We therefore investi-

gated hypoxia-induced cell death in LN-18 and LN-229 cells transfected with BCL-X<sub>L</sub>: enhanced expression of BCL-X<sub>L</sub> conferred significant protection from hypoxia-induced cell death in both cell lines. Results for LN-18 cells are shown in Figure 7a (note that the difference between LN-18 neo and LN-18 BCL-X<sub>L</sub> was not statistically significant at H20). However, BCL-X<sub>L</sub> did not prevent hypoxia-induced ATP depletion (results for LN-18 cells are shown in Figure 7a). This is compatible with anaerobic extramitochondrial ATP generation under hypoxia and a model where mitochondrial injury might be a consequence of energy depletion rather than its cause.

To further characterize the role of inhibitors of apoptosis, LN-229 cells were transduced with a vector encoding the X-linked-inhibitor-of-apoptosis-protein (XIAP) or a green fluorescent protein (GFP) control vector by adenoviral gene transfer. While XIAP protected cells from CD95L-induced apoptosis under normoxia (Figure 7b, left), it did not protect against hypoxic cell death. To ascertain proper function of the adenovirally transferred XIAP also under hypoxic conditions, we exposed the cells to hypoxia in the presence of CD95L: XIAP was protective solely against the additional cell death caused by CD95L (Figure 7b, right).

Similar, ectopic expression of the viral caspase 8 inhibitor cytokine response modifier-A (crm-A) in LN-229 cells did not confer protection from hypoxic cell death, while efficiently inhibiting CD95 ligand-induced apoptosis (Figure 7c). Despite the lack of detectable caspase cleavage, incubation of LN-18 cells with the broad spectrum protease inhibitor zVAD-fmk conferred protection against hypoxic cell death (Figure 7d). In contrast, the more specific inhibitors of caspases 3 and 9, zDEVD-fmk and zLEHD-fmk, respectively, did not protect against hypoxia-induced cell death (Figure 7d). The effect of zVAD-fmk was already detectable immediately following hypoxia, with no additional protection generated during normoxic recovery, and similar data were obtained in LN-229 cells (not shown).

## Discussion

Here we have characterized the features of hypoxic cell death of malignant glioma cell lines *in vitro* in a paradigm of profound hypoxia and partial glucose deprivation. In contrast to classical apoptotic cell death induced by hypoxia in E1A and Ha-*ras*-transformed cell lines,<sup>12</sup> several nonglioma tumor cell lines<sup>13,14</sup> and nontransformed cells,<sup>15</sup> only early morphological features of apoptosis, but predominant necrosis, became evident by ultrastructural and biochemical analysis in the glioma cell lines. Since the glioma cells investigated in this study are proficient to undergo caspase activation and apoptosis in response to death ligands or cytotoxic drugs,<sup>33</sup> specific mechanisms must account for the absence of hypoxia-induced apoptosis. Antiapoptotic molecules expressed by glioma cells may prevent hypoxic stimuli from activating the cell death program as long as energy resources and organelle integrity are preserved. Ultimately, cell death ensues when the available nutrients, for example, glucose, are consumed, and cellular ATP is progressively depleted.<sup>30</sup> This notion is supported by the protection of the glioma cell

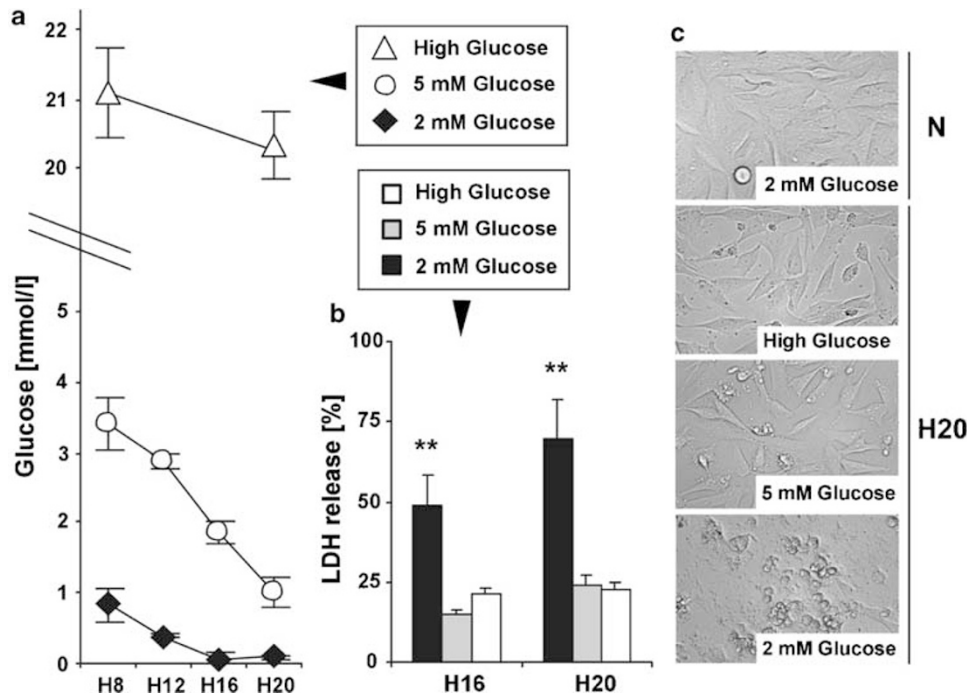


**Figure 5** Glucose protects glioma cells from hypoxia-induced cell death. LN-229 cells were exposed to hypoxia in the presence of 2 and 5 mM glucose or serum-free medium (25 mM glucose). (a) Glucose concentration was analyzed immediately following hypoxia. (b) In a parallel assay, cell death was assessed by LDH release after 24 h of normoxic recovery (\*\* $P < 0.01$  for the comparison of 2 mM Glucose versus 5 mM glucose and 25 mM glucose, student's *t*-test). (c) Phase contrast images of LN-229 cells exposed to hypoxia (H20) or normoxia (N) for 20 h in the presence of 2 and 5 mM glucose or serum-free medium (25 mM glucose) followed by 24 h of normoxic recovery

lines from hypoxia-induced cell death by higher concentrations of glucose, as described earlier for kidney cells<sup>37</sup> and astrocytes.<sup>38</sup> Consistent with this model, cells surviving shorter periods of hypoxia were able to recover and reconstitute normal ATP levels, without the occurrence of delayed cell death. However, once ATP levels were profoundly depleted, progressive cell death ensued even during normoxic incubation with glucose replenishment (Figure 4). Disruption of mitochondria is likely to account for the inability of cells to recover from these conditions.<sup>37</sup> However, it is notable that delayed cell death following reconstitution of ATP levels after mitochondrial injury in other models is apoptotic.<sup>30,37</sup>

In most paradigms of apoptosis, cytochrome *c* release results in the formation of a complex, the apoptosome, involving caspase 9 and apoptotic protease activating factor 1 (APAF 1), leading to the cleavage of caspase 9 and subsequently apoptotic cell death. However, ATP is required for the cleavage of caspase 9 by the apoptosome.<sup>39,40</sup> Under conditions of energy failure, caspase 9 activation and subsequent effector caspase activation may be incomplete.<sup>41</sup> This mechanism in conjunction with the expression of apoptosis-inhibitory proteins of the inhibitor-of-apoptosis-protein (IAP) and BCL-2 family<sup>42,43</sup> may explain the absence of caspase cleavage and end stages of apoptosis in our paradigm. However, if there is no caspase cleavage, why does zVAD-fmk protect against hypoxia-induced cell death? Since neither XIAP, which acts on both caspases 3 and 8, nor crm-A, which acts predominantly on caspase 8, or the more specific caspase inhibitors zDEVD-fmk and zLEHD-fmk alter

hypoxia-induced cell death, the protection provided by zVAD-fmk may be related to the inhibition of caspases other than 3, 7, 8 or 9, or to effects of zVAD-fmk on noncaspase proteases. With regard to this possibility, it is well recognized that zVAD does not exclusively inhibit caspases (for review of other proteases and references for noncaspase-specific actions of zVAD.fmk see Leist and Jaattela<sup>44</sup>). Indeed, inhibition of calpain, the activation of which contributes to necrosis during hypoxic-hypoglycemic-injury (reviewed in Wang<sup>45</sup>) by zVAD-fmk, has been observed.<sup>46</sup> We have also considered the possibility of secondary necrosis in our system, which can especially occur following failed apoptosis, for the changes observed following hypoxia and additional normoxic recovery. However, since there was no detectable apoptosis by morphological and biochemical criteria also immediately following hypoxia even at the shortest incubation times resulting in detectable cell death, we dismissed this notion.

Hypoxic cell death in glioma cells resembles death induced by cytotoxic drugs, staurosporine or UV light in APAF 1 knockout embryonic stem cells which undergo nonapoptotic caspase-independent cell death. BCL-2 protects APAF 1 knockout cells by preserving mitochondrial membrane potential independent from caspase activation.<sup>47</sup> The protection afforded by ectopic BCL-X<sub>L</sub> expression in our experiments is therefore probably caused by stabilization of mitochondria against hypoxia-induced damage.<sup>37,47,48</sup> APAF 1- and caspase 3-independent cell death may comprise peripheral chromatin condensation (stage I) similar to our results, in the absence of oligonucleosomal DNA fragmentation. Release of apoptosis inducing factor (AIF) from mitochondria

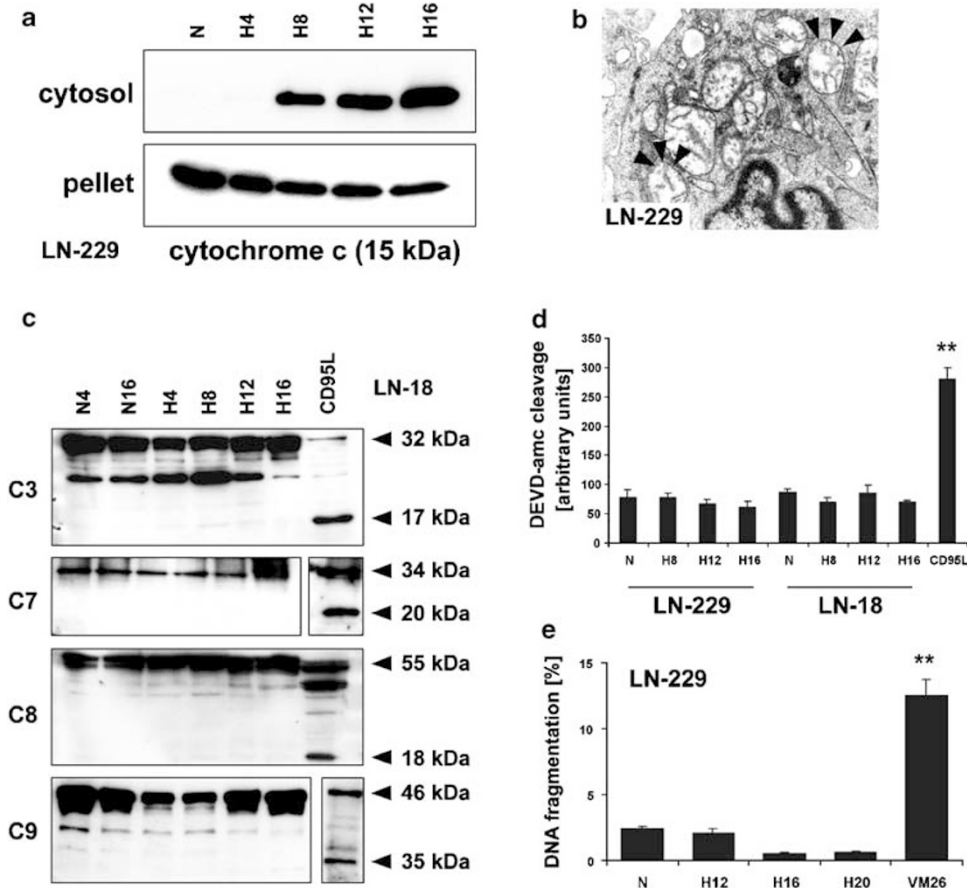


**Figure 6** Hypoxia induces mitochondrial injury, but no caspase cleavage or DNA fragmentation. (a) After exposure to normoxia or hypoxia, LN-229 cells were permeabilized with digitonin, and the release of mitochondrial cytochrome *c* was detected by immunoblot of cytoplasmic proteins. The mitochondrial cytochrome *c* was analyzed by immunoblot of the pellet fraction. (b) LN-229 cells were exposed to hypoxia for 8 h and immediately thereafter prepared for electron microscopy. Note the mitochondrial swelling with distension of the cristae (arrowheads). (c) Immunoblots of lysates from LN-18 cells exposed to hypoxia for the times indicated and lysed immediately thereafter was performed with antibodies to caspases 3, 7, 8 or 9. CD95L-treated cells were used as positive control. Note the additional band in blots incubated with antibody to caspase 3, which may correspond to a band of approximately 24 kDa that is frequently observed in these cells, and is thought to correspond to an inactive intermediate form of caspase 3 processing. (d) LN-229 and LN-18 cells were exposed to normoxia (N) or hypoxia for 8–16 h. DEVD-amc cleavage (expressed in arbitrary units of fluorescence) was determined by fluorimetry (\*\* $P < 0.01$ , Student's *t*-test). CD95L-treated cells were used as positive control. (e) LN-229 cells were exposed to normoxia or hypoxia for 12–20 h followed by 24 h of normoxic recovery. DNA fragmentation was assessed by fluorimetry (\*\* $P < 0.01$ , Student's *t*-test). Teniposide (VM26)-treated cells were employed as a positive control (C3, C7, C8, C9: caspases 3, 7, 8, 9)

may act as the critical effector for this phenomenon.<sup>49</sup> The primary cause of hypoxia-induced mitochondrial injury is unclear. Possibly, ATP depletion itself leads to loss of mitochondrial membrane potential and the observed morphological alterations. Cytochrome *c* released from mitochondria may then cause an arrest of electron transport within the respiratory chain, resulting in the production of membrane-damaging free radicals and cessation of mitochondrial ATP production, further paving the way towards cell death.<sup>50</sup>

In contrast to paradigms where a death stimulus is applied and only the mode of cell death is ATP-dependent, hypoxia *per se* might not be a sufficient death stimulus in this system. Therefore, we consider energy deprivation as the possible primary cause of cell death in contrast to the models studied by Leist *et al.*<sup>30</sup> and others, on which the concept of ATP as a molecular switch between apoptosis and necrosis is based.

Caspase-independent death of cancer cells is increasingly recognized as an important mechanism with implications for the development of novel cancer therapies. Our findings

correspond to the predominance of necrosis over apoptosis in human glioblastoma *in vivo* despite extensive hypoxia,<sup>7,16</sup> and it appears likely that our model mimics the conditions faced by many tumor cells in the microenvironment of human glioblastoma. Further, the sensitivity of glioma cells to the induction of apoptosis by hypoxia may be important for antiangiogenic therapies, which in other solid tumors so far have had disappointing results in clinical trials. Insight into the mechanisms opposing hypoxia-induced apoptosis may result in strategies to sensitize tumor cells to hypoxia and enhance the impact of antiangiogenic therapy. Finally, this model will be valuable for the study of the effects of other therapies aiming to induce cell death in the hypoxic tumor cell fraction.

## Materials and Methods

### Reagents and cell lines

*N*-acetyl-Asp-Glu-Val-Asp-7-methyl-4-aminocoumarin (DEVD-amc), *Z*-Val-Ala-Asp-fluoromethylketone (zVAD-fmk) and *Z*-Leu-Glu-His-Asp-7-methyl-

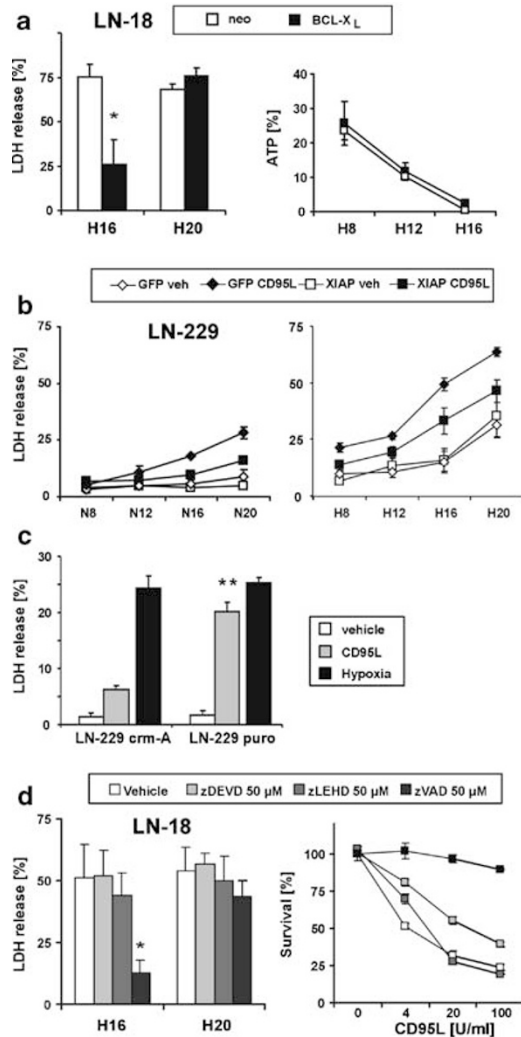


**Figure 7** BCL-X<sub>L</sub> confers protection from hypoxia-induced cell death without altering ATP-levels. (a) LN-18 cells engineered to overexpress BCL-X<sub>L</sub> were exposed to normoxia or hypoxia and analyzed for cytotoxicity by LDH assay after 24 h of normoxic recovery (\**P* < 0.05 for the comparison of neo versus BCL-X<sub>L</sub> cells at 16 h, Student's *t*-test) and for ATP immediately following hypoxia (\**P* < 0.05 for the comparison of neo versus BCL-X<sub>L</sub> cells at 16 h and 20 h, student's *t*-test). (b) LN-229 cells were transduced with XIAP or GFP by adenoviral gene transfer. At 24 h after infection, cells were exposed to hypoxia or normoxia in the presence of CD95L (100 U/ml) or vehicle. Cytotoxicity was assessed by LDH assay. (c) LN-229 crm-A cells or LN-229 puro control cells were incubated under normoxia or hypoxia for 12 h. As a positive control for inhibition of caspase 8-dependent cell death by crm-A, cells were incubated with 100 U/ml CD95L under normoxia (\*\**P* < 0.001 for the comparison of crm-A versus puro cells following treatment with CD95L under normoxia, student's *t*-test). (d) LN-18 cells were exposed to normoxia or hypoxia in the presence of 50 μM zVAD-fmk, 50 μM zDEVD-fmk, 50 μM zLEHD-fmk or vehicle. Immediately following hypoxia, cell death was assessed by LDH release assay (\**P* < 0.05 for the comparison of vehicle versus zVAD-fmk, student's *t*-test). In a parallel experiment, LN-18 cells were exposed to CD95L in the presence of 50 μM zVAD-fmk, zDEVD-fmk, zLEHD-fmk or vehicle for 24 h. Survival was assessed by crystal violet staining

4-fluoromethylketone (zLEHD-fmk) were obtained from Bachem (Heidelberg, Germany). Z-Asp-Glu-Val-Asp-7-methyl-4-fluoromethylketone (zDEVD-fmk) was obtained from Calbiochem (Schwalbach, Germany). Teniposide (VM26) was obtained from Bristol (Munich,

Germany). All other chemicals not specified below were purchased from Sigma (Deisenhofen, Germany). CD95 ligand (CD95L) was obtained from the supernatant of CD95L-transfected N2A murine neuroblastoma cells.<sup>51</sup> LN-18 (p53 mutant), LN-229 and U87MG (both p53 wildtype) human malignant glioma cell lines have been characterized previously.<sup>43</sup> LN-18 and LN-229 cells transfected with the pSFFV-BCL-X<sub>L</sub> construct or an empty neo control vector have been described.<sup>36</sup> LN-229 crm-A cells were obtained using the Flag-crm-A-puro construct and were compared with puromycin-resistant control cells transfected with the empty vector.

Adenoviral gene transfer of XIAP was performed as described.<sup>42</sup> Briefly, cells were infected with XIAP-adenovirus or GFP control adenovirus at a multiplicity of infection (MOI) of 300. At 24 h after infection, the virus-containing supernatant was removed and cells were incubated under hypoxic or normoxic conditions for the times indicated. Cell death was assessed immediately following hypoxia by LDH-assay.

The glioma cells were maintained in DMEM containing 10% fetal calf serum, 2 mM glutamine, 100 IU/ml penicillin and 100 mg/ml streptomycin.

## Induction of hypoxia

Cells were plated on glass petri dishes of various sizes with cell density adjusted to  $5 \times 10^5$  cells/cm<sup>2</sup> or on glass 96-well plates (Hellma, Mühlheim, Germany) at a density of  $2.5 \times 10^4$ /well and allowed to attach in medium containing 10% fetal calf serum for 24 h. Then the medium was removed and the cells were incubated in serum-free DMEM without glucose (Gibco BRL, Basel, Switzerland) adjusted to 2 mM glucose under normoxia or hypoxia. The experimental conditions have been described previously.<sup>52,53</sup> Briefly, the cells were incubated in sealed chambers exposed to a mixture of 200 ppm O<sub>2</sub>, 5% CO<sub>2</sub> and 95% argon or normoxic control conditions in a humidified atmosphere. After hypoxia for the times indicated, the cells were allowed to recover for 24 h with replenishment of glucose to 12.5 mM and addition of 1% fetal calf serum. For some experiments, the cells were prepared for analysis either immediately after hypoxia or after the 24 h recovery period. No decrease in pH < 7.2 occurred under these conditions. Alternatively, hypoxia was induced chemically by incubating the plates in Gas Pak pouches for anaerobic culture (Becton Dickinson, Heidelberg, Germany).<sup>54</sup> This procedure results in hypoxia of less than 0.4% O<sub>2</sub> with 4–10% of CO<sub>2</sub> after 100 min. The Gas Pak technique was extensively characterized and yielded identical results compared to gassing with 0.02% O<sub>2</sub> with 5% CO<sub>2</sub> as judged by LDH release assay, caspase cleavage, glucose and ATP depletion and ultrastructural features of cell death.

## Electron microscopy

Glioma cells grown in 60 mm plates and treated as indicated were fixed in 2.5% glutaraldehyde (Paesel-Lorei, Frankfurt, Germany) in Hank's modified salt solution (HMSS), postfixed in 1% OsO<sub>4</sub> in 0.1 M cacodylate buffer, scraped off the plastic and dehydrated in ethanol. The 70% ethanol step was saturated with uranyl acetate for contrast enhancement. Dehydration was completed in propylene oxide. The specimens were embedded in Araldite (Serva, Heidelberg, Germany). Ultrathin sections were produced on an FCR Reichert Ultracut ultramicrotome (Leica, Bensheim, Germany), mounted on pioloform-coated copper grids and contrasted with lead citrate. Specimens were analyzed and documented with an EM 10A electron microscope (Zeiss, Oberkochen, Germany).

## Viability assays

The cells were seeded in 96-well plates and allowed to attach for 24 h. The cells were exposed to hypoxia or normoxia and treated as indicated. Immediately following hypoxia or after recovery under normoxia, the plates were centrifuged, and the LDH concentration in the supernatant was assessed employing the cell death detection kit II (Boehringer Mannheim, Mannheim, Germany). Crystal violet staining was performed as described.<sup>51</sup>

## DEVD-amc-cleaving caspase activity

The cells were seeded in 96-well plates and allowed to attach for 24 h. The cells were exposed to hypoxia or normoxia and lysed immediately after hypoxia in buffer containing 25 mM Tris-HCl (pH 8.0), 60 mM NaCl, 2.5 mM EDTA and 0.25% NP40 for 10 min. DEVD-amc (12.5  $\mu$ M) diluted in PBS was added and incubated at 37°C for 10 min. Caspase activity was measured for 1 h using a CytoFluor 2350 Millipore fluorimeter at 360 nm excitation and 480 nm emission wavelengths.

## DNA fragmentation assay

The cells were grown in 60 mm plates, allowed to attach for 24 h and exposed to hypoxia or normoxia. After normoxic recovery, the cells were pelleted by centrifugation (7 min, 1200 rpm, 4°C). The pellet was dissolved in lysis buffer (10 mM Tris-HCl, pH 7.5, 10 mM EDTA, 0.2% Triton X-100) and lysed for 10 min at 4°C. The lysates were centrifuged at 13 000 rpm and 4°C. Supernatant was taken for the measurement of fragmented DNA. The pellet with the intact DNA was again dissolved in lysis buffer and sonified for 20 s. RNase (100  $\mu$ g/ml) was added to all samples. RNA was digested for 2 h at 37°C. All samples were diluted in buffer containing 5 mM TRIS-HCl, pH 7.5, 0.5 mM EDTA and 0.5  $\mu$ g/ml ethidium bromide and measured for the content of DNA using a CytoFluor 2350 Millipore fluorimeter at 530 nm excitation and 620 nm emission wavelengths.

## Immunoblot analysis

The cells were grown on 60 mm plates. Immediately after hypoxia or normoxia, the cells were washed with cold PBS, harvested into ice-cold PBS containing phenylmethyl-sulfonylfluoride (PMSF) (10  $\mu$ g/ml) with a cell scraper, lysed in lysis buffer containing 50 mM Tris-HCl, pH 8, 120 mM NaCl, 0.5% NP-40, 100  $\mu$ g/ml PMSF, 10  $\mu$ g/ml leupeptin and 2  $\mu$ g/ml aprotinin, for 15 min on ice and centrifuged at 13 000 rpm for 10 min at 4°C. The protein concentration was determined by the Bio-Rad Protein Assay (Bio-Rad, Munich, Germany). Soluble proteins (20  $\mu$ g/lane) were separated by SDS-PAGE and blotted to nitrocellulose by standard procedures. Equal loading was ascertained by Ponceau S staining. The membranes were pretreated for 2 h with PBS containing 5% skim milk, 0.05% Tween 20 and then incubated for 16 h at 4°C with antibodies to caspase 3, BCL-X<sub>L</sub> (Transduction Laboratories, Lexington, KY, USA), caspases 7, 9 (kindly supplied by Dr. Y Lazebnik, Cold Spring Harbor, NY, USA), caspase 8 (kindly supplied by Dr. PH Krammer, Heidelberg, Germany), BCL-2 (PharMingen, San Diego, CA, USA), BAX and actin (Santa Cruz, San Diego, CA, USA). The secondary antibodies, protein A and anti-mouse IgG, were purchased from Amersham (Braunschweig, Germany), anti-goat antibody was from Santa Cruz. Enhanced chemiluminescence (ECL+, Amersham) was used for detection.

## Cytochrome c release assay

The cells were grown in 100 mm plates. After hypoxia and immediately following recovery under normoxia, the cells were washed with PBS and cytoplasmic cytochrome *c* was extracted by permeabilization with mannitol, sucrose, HEPES (MSH) buffer plus digitonin (210 mM D-mannitol, 70 mM sucrose, 10 mM HEPES, 200  $\mu$ M EGTA, 5 mM succinate, 0.15% BSA, 40  $\mu$ g/ml digitonin) at 4°C. After lysis, the supernatant was removed and centrifuged immediately for 10 min at 13 000  $\times$  g. An equal volume of 10% trichloroacetic acid was added to the supernatant. Samples were kept at -20°C for at least 30 min. After another centrifugation (15 min at 13000  $\times$  g), the pellets were dissolved in sample buffer (50 mM TRIS-HCl, pH 6.8, 2% SDS, 0.1% bromophenolblue, 10% glycerol) and analyzed for cytochrome *c* content by SDS-PAGE and immunoblot, employing mouse monoclonal cytochrome *c* antibody from PharMingen (San Diego, CA, USA). The mitochondrial cytochrome *c* content was analyzed by SDS-PAGE from the pellet fraction.

## Annexin V binding assay

The cells were exposed to hypoxia or normoxia as described above. Immediately after hypoxia, or after 24 h recovery as specified, the cells were washed and stained with propidium iodide and Annexin V (Becton Dickinson PharMingen, Heidelberg, Germany) according to the instructions of the manufacturer. Specific binding was analyzed by FACS utilizing a Becton Dickinson FACSCalibur and the Cell Quest software.

## ATP assay

The cells were exposed to hypoxia or normoxia as described above. Immediately after hypoxia, or after 24 h recovery as specified, the plates were placed on ice, and the cells were pelleted by centrifugation and lysed in ATP releasing agent (Sigma). ATP was determined by luciferase assay with the CLS II kit (Boehringer Mannheim, Mannheim, Germany).<sup>30</sup> Typical absolute values for normoxic control cells grown in serum-free medium containing 2 mM glucose were in the region of 2.8 nM ATP/mg protein. Values were normalized for LDH release to detect the ATP levels in surviving cells and are given in percentage of values in normoxic control cells. There was no decline in ATP levels >15% for up to 20 h of normoxia with serum-free medium and 2 mM glucose (not shown).

## Glucose assay

The cells were exposed to hypoxia or normoxia as described above. Immediately after hypoxia, the cells were pelleted by centrifugation and the glucose concentration in the supernatant was determined employing the Gluco-quant Glucos/HK Kit (Roche, Basel, Switzerland).

## Statistical analysis

Data are commonly representative of three independent experiments with similar results. Quantitative data are expressed as means and S.D. of triplicate experiments and were assessed for significance by Student's *t*-test.

## Acknowledgements

This study was supported by a grant from the German Cancer Council (10-1802-We 5) to MW and a grant from the *fortune* program of the University of Tübingen to JS (724-0-0). We thank P Supra for excellent technical



assistance, and H-J Riedinger and G Probst for help with the experimental setup for hypoxic incubation.

## References

- Ramplung R, Cruickshank G, Lewis AD, Fitzsimmons SA and Workman P (1994) Direct measurement of pO<sub>2</sub> distribution and bioreductive enzymes in human malignant brain tumors. *Int. J. Radiat. Oncol. Biol. Phys.* 29: 427–431
- Valk PE, Mathis CA, Prados MD, Gilbert JC and Budinger TF (1992) Hypoxia in human gliomas: demonstration by PET with fluorine-18- fluoromisonidazole. *J. Nucl. Med.* 33: 2133–2137
- Collingridge DR, Piepmeier JM, Rockwell S and Knisely JP (1999) Polarographic measurements of oxygen tension in human glioma and surrounding peritumoural brain tissue. *Radiother. Oncol.* 53: 127–131
- Zagzag D, Amirnovin R, Greco MA, Yee H, Holash J, Wiegand SJ, Zabski S, Yancopoulos GD and Grumet M (2000) Vascular apoptosis and involution in gliomas precede neovascularization: a novel concept for glioma growth and angiogenesis. *Lab. Invest.* 80: 837–849
- Holash J, Maisonpierre PC, Compton D, Boland P, Alexander CR, Zagzag D, Yancopoulos GD and Wiegand SJ (1999) Vessel cooption, regression, and growth in tumors mediated by angiopoietins and VEGF. *Science* 284: 1994–1998
- Royds JA, Dower SK, Qwarnstrom EE and Lewis CE (1998) Response of tumour cells to hypoxia: role of p53 and NFκB. *Mol. Pathol.* 51: 55–61
- Kleihues P, Burger PC, Collins VP, Newcomb EW, Ohgaki H and Cavenee WK (2000) Glioblastoma. In *Pathology and Genetics of Tumours of the Nervous System*, Kleihues P and Cavenee WK (eds) (Lyon: IARC Press) pp. 29–39
- Kimura H, Braun RD, Ong ET, Hsu R, Secomb TW, Papahadjopoulos D, Hong K and Dewhirst MW (1996) Fluctuations in red cell flux in tumor microvessels can lead to transient hypoxia and reoxygenation in tumor parenchyma. *Cancer Res.* 56: 5522–5528
- Helmlinger G, Yuan F, Dellian M and Jain RK (1997) Interstitial pH and pO<sub>2</sub> gradients in solid tumors *in vivo*: high-resolution measurements reveal a lack of correlation. *Nat. Med.* 3: 177–182
- Read TA, Sorensen DR, Mahesparan R, Enger PO, Timpl R, Olsen BR, Hjelstuen MH, Haraldseth O and Bjerkvig R (2001) Local endostatin treatment of gliomas administered by microencapsulated producer cells. *Nat. Biotechnol.* 19: 29–34
- Machein MR, Risau W and Plate KH (1999) Antiangiogenic gene therapy in a rat glioma model using a dominant-negative vascular endothelial growth factor receptor 2. *Hum. Gene Ther.* 10: 1117–1128
- Graeber TG, Osmanian C, Jacks T, Housman DE, Koch CJ, Lowe SW and Giaccia AJ (1996) Hypoxia-mediated selection of cells with diminished apoptotic potential in solid tumours. *Nature* 379: 88–91
- Araya R, Uehara T and Nomura Y (1998) Hypoxia induces apoptosis in human neuroblastoma SK-N-MC cells by caspase activation accompanying cytochrome *c* release from mitochondria. *FEBS Lett.* 439: 168–172
- Amellem O, Stokke T, Sandvik JA, Smedshammer L and Pettersen EO (1997) Hypoxia-induced apoptosis in human cells with normal p53 status and function, without any alteration in the nuclear protein level. *Exp. Cell Res.* 232: 361–370
- Saikumar P, Dong Z, Weinberg JM and Venkatachalam MA (1998) Mechanisms of cell death in hypoxia/reoxygenation injury. *Oncogene* 17: 3341–3349
- Tohma Y, Gratas C, Van Meir EG, Desbaillets I, Tenan M, Tachibana O, Kleihues P and Ohgaki H (1998) Necrogenesis and Fas/APO-1 (CD95) expression in primary (*de novo*) and secondary glioblastomas. *J. Neuropathol. Exp. Neurol.* 57: 239–245
- Steinbach JP and Weller M (2002) Mechanisms of apoptosis in CNS tumors: application to theory. *Curr. Neurol. Neurosci. Rep.* 2: 246–253
- Tachibana O, Lampe J, Kleihues P and Ohgaki H (1996) Preferential expression of Fas/APO1 (CD95) and apoptotic cell death in perinecrotic cells of glioblastoma multiforme. *Acta Neuropathol.* 92: 431–434
- Schiffer D, Cavalla P, Migheli A, Chio A, Giordana MT, Marino S and Attanasio A (1995) Apoptosis and cell proliferation in human neuroepithelial tumors. *Neurosci. Lett.* 195: 81–84
- Plate KH, Breier G, Weich HA and Risau W (1992) Vascular endothelial growth factor is a potential tumour angiogenesis factor in human gliomas *in vivo*. *Nature* 359: 845–848
- Dong Z, Venkatachalam MA, Wang J, Patel Y, Saikumar P, Semenza GL, Force T and Nishiyama J (2001) Up-regulation of apoptosis inhibitory protein IAP-2 by hypoxia. Hif-1-independent mechanisms. *J. Biol. Chem.* 276: 18702–18709
- Kim CY, Tsai MH, Osmanian C, Graeber TG, Lee JE, Giffard RG, DiPaolo JA, Peehl DM and Giaccia AJ (1997) Selection of human cervical epithelial cells that possess reduced apoptotic potential to low-oxygen conditions. *Cancer Res.* 57: 4200–4204
- Teicher BA (1994) Hypoxia and drug resistance. *Cancer Metast. Rev.* 13: 139–168
- Hockel M, Vormdran B, Schlenger K, Baussmann E and Knapstein PG (1993) Tumor oxygenation: a new predictive parameter in locally advanced cancer of the uterine cervix. *Gynecol. Oncol.* 51: 141–149
- Korshunov A, Golanov A, Sycheva R and Pronin I (1999) Prognostic value of tumour associated antigen immunoreactivity and apoptosis in cerebral glioblastomas: an analysis of 168 cases. *J. Clin. Pathol.* 52: 574–580
- Rhodes RH (1998) Biological evaluation of biopsies from adult cerebral astrocytomas: cell-growth/cell-suicide ratios and their relationship to patient survival. *J. Neuropathol. Exp. Neurol.* 57: 746–757
- Hossmann KA, Mies G, Paschen W, Szabo L, Dolan E and Wechsler W (1986) Regional metabolism of experimental brain tumors. *Acta Neuropathol.* 69: 139–147
- Mies G, Paschen W, Ebhardt G and Hossmann KA (1990) Relationship between blood flow, glucose metabolism, protein synthesis, glucose and ATP content in experimentally induced glioma (RG1 2.2) of rat brain. *J. Neurooncol.* 9: 17–28
- Vaupel P (1992) Physiological properties of malignant tumours. *NMR Biomed.* 5: 220–225
- Leist M, Single B, Castoldi AF, Kuhnl S and Nicotera P (1997) Intracellular adenosine triphosphate (ATP) concentration: a switch in the decision between apoptosis and necrosis. *J. Exp. Med.* 185: 1481–1486
- Eguchi Y, Shimizu S and Tsujimoto Y (1997) Intracellular ATP levels determine cell death fate by apoptosis or necrosis. *Cancer Res.* 57: 1835–1840
- Weller M, Frei K, Groscurth P, Krammer PH, Yonekawa Y and Fontana A (1994) Anti-Fas/APO-1 antibody-mediated apoptosis of cultured human glioma cells. Induction and modulation of sensitivity by cytokines. *J Clin Invest* 94: 954–964
- Glaser T, Wagenknecht B, Groscurth P, Krammer PH and Weller M (1999) Death ligand/receptor-independent caspase activation mediates drug-induced cytotoxic cell death in human malignant glioma cells. *Oncogene* 18: 5044–5053
- Hermisson M, Wagenknecht B, Wolburg H, Glaser T, Dichgans J and Weller M (2000) Sensitization to CD95 ligand-induced apoptosis in human glioma cells by hyperthermia involves enhanced cytochrome *c* release. *Oncogene* 19: 2338–2345
- Gerweck LE, Seneviratne T and Gerweck KK (1993) Energy status and radiobiological hypoxia at specified oxygen concentrations. *Radiat Res* 135: 69–74
- Glaser T, Wagenknecht B and Weller M (2001) Identification of p21 as a target of cycloheximide-mediated facilitation of CD95-mediated apoptosis in human malignant glioma cells. *Oncogene* 20: 4757–4767
- Saikumar P, Dong Z, Patel Y, Hall K, Hopper U, Weinberg JM and Venkatachalam MA (1998) Role of hypoxia-induced Bax translocation and cytochrome *c* release in reoxygenation injury. *Oncogene* 17: 3401–3415
- Callahan DJ, Engle MJ and Volpe JJ (1990) Hypoxic injury to developing glial cells: protective effect of high glucose. *Pediatr. Res.* 27: 186–190
- Li P, Nijhawan D, Budihardjo I, Srinivasula SM, Ahmad M, Alnemri ES and Wang X (1997) cytochrome *c* and dATP-dependent formation of Apaf-1/caspase-9 complex initiates an apoptotic protease cascade. *Cell* 91: 479–489
- Slee EA, Harte MT, Kluck RM, Wolf BB, Casiano CA, Newmeyer DD, Wang HG, Reed JC, Nicholson DW, Alnemri ES, Green DR and Martin SJ (1999) Ordering the cytochrome *c*-initiated caspase cascade: hierarchical activation of caspases-2, -3, -6, -7, -8, and -10 in a caspase-9- dependent manner. *J. Cell Biol.* 144: 281–292
- Eguchi Y, Srinivasan A, Tomaselli KJ, Shimizu S and Tsujimoto Y (1999) ATP-dependent steps in apoptotic signal transduction. *Cancer Res.* 59: 2174–2181

42. Wagenknecht B, Glaser T, Naumann U, Kugler S, Isenmann S, Bahr M, Korneluk R, Liston P and Weller M (1999) Expression and biological activity of X-linked inhibitor of apoptosis (XIAP) in human malignant glioma. *Cell Death Differ* 6: 370–376
43. Weller M, Rieger J, Grimm C, Van Meir EG, De Tribolet N, Krajewski S, Reed JC, von Deimling A and Dichgans J (1998) Predicting chemoresistance in human malignant glioma cells: the role of molecular genetic analyses. *Int. J. Cancer* 79: 640–644
44. Leist M and Jaattela M (2001) Four deaths and a funeral: from caspases to alternative mechanisms. *Nat Rev Mol Cell Biol* 2: 589–598
45. Wang KK (2000) Calpain and caspase: can you tell the difference? *Trends Neurosci* 23: 20–26
46. Waterhouse NJ, Finucane DM, Green DR, Elce JS, Kumar S, Alnemri ES, Litwack G, Khanna K, Lavin MF and Watters DJ (1998) Calpain activation is upstream of caspases in radiation-induced apoptosis. *Cell Death Differ* 5: 1051–1061
47. Haraguchi M, Torii S, Matsuzawa S, Xie Z, Kitada S, Krajewski S, Yoshida H, Mak TW and Reed JC (2000) Apoptotic protease activating factor 1 (Apaf-1)-independent cell death suppression by Bcl-2. *J Exp Med* 191: 1709–1720
48. Green DR and Reed JC (1998) Mitochondria and apoptosis. *Science* 281: 1309–1312
49. Susin SA, Dugas E, Ravagnan L, Samejima K, Zamzami N, Loeffler M, Costantini P, Ferri KF, Irinopoulou T, Prevost MC, Brothers G, Mak TW, Penninger J, Earnshaw WC and Kroemer G (2000) Two distinct pathways leading to nuclear apoptosis. *J Exp Med* 192: 571–580
50. Reed JC (1997) cytochrome c: can't live with it—can't live without it. *Cell* 91: 559–562
51. Roth W, Fontana A, Trepel M, Reed JC, Dichgans J and Weller M (1997) Immunochemotherapy of malignant glioma: synergistic activity of CD95 ligand and chemotherapeutics. *Cancer Immunol. Immunother.* 44: 55–63
52. Probst H, Schiffer H, Gekeler V, Kienzle Pfeilsticker H, Stropp U, Stotzer KE and Frenzel-Stotzer I (1988) Oxygen dependent regulation of DNA synthesis and growth of Ehrlich ascites tumor cells *in vitro* and *in vivo*. *Cancer Res.* 48: 2053–2060
53. Dreier T, Scheidtmann KH and Probst H (1993) Synchronous replication of SV 40 DNA in virus infected TC 7 cells induced by transient hypoxia. *FEBS Lett.* 336: 445–451
54. Kendler A and Dawson G (1990) Progressive hypoxia inhibits the de novo synthesis of galactosylceramide in cultured oligodendrocytes. *J Biol Chem* 265: 12259–12266